International Journal of Nanoscience
Vol. 3, Nos. 4 & 5 (2004) 631–638

World Scientific
www.worldscientific.com

SYNTHESIS OF Fe NANOPARTICLES BY REDOX REACTION USING AN ELECTRON BEAM DEPOSITION TECHNIQUE

S. JAIN*, S. Y. CHAN†, A. O. ADEYEYE*,§ and C. B. BOOTHROYD‡

*Information Storage Materials Laboratory
Department of Electrical and Computer Engineering
4 Engineering Drive 3, National University of Singapore, Singapore 117576
†Data Storage Institute, DSI Building 5, Engineering Drive 1, Singapore 117608
‡Institute of Materials Research and Engineering, 3 Research Link, Singapore
§eleaao@nus.edu.sg

A new technique for synthesizing Fe nanoparticles based on an electron beam deposition technique from a Fe_2O_3 source has been developed. We deposited Fe_2O_3 films directly on Si(001) substrates, Al and Cu buffer layer, and observed the formation of Fe nanoparticles at the Si(001) and Al interfaces respectively. The Al at the interface is oxidized to Al_2O_3 and Si is oxidized to SiO_2. For films deposited on Cu buffer layer, however, no Fe nanoparticles were formed. We explain our results in terms of the enthalpy of formation of the oxides. The enthalpy of formation of SiO_2 and Al_2O_3 is much lower than that of Fe_2O_3, thus promoting the formation of Fe nanoparticles. The enthalpy of formation of CuO is however, greater than that of Fe_2O_3 thus forbidding the formation of Fe nanoparticles. This is in agreement with both X-ray Photoelectron Spectroscopy (XPS) depth profile analysis and Transmission Electron Microscopy (TEM).

Keywords: Fe nanoparticles.

1. Introduction

Thin iron oxide films have been the subject of many studies, primarily due to their interesting magnetic properties and technological applications.[1–5] These films can exhibit several crystal structures and compositions owing to the different possible valence states of the iron cations. Fe_2O_3 is of particular interest because of its applications in magnetic recording media.[6] Current research efforts are focused on the fabrication of Fe nanomaterials and to exploit its special magnetic properties. Numerous nanofabrication techniques have been developed to synthesize a wide variety of magnetic nanoparticles. S. Gangopadhyay *et al.*[7] for example, developed a method for synthesizing ultrafine particles of Fe by evaporation and condensation of the bulk metal in an inert atmosphere. In another method by Y. Li *et al.*,[8] high precision alignment of iron nanoparticles was accomplished using Scanning Tunneling Microscopy (STM) assisted by chemical vapor deposition to grow the particles.

§Corresponding author.

Table 1. Film structures of the various templates used in the experiments.

Sample	Film structure
A	Si(001)/Fe_2O_3 (200 nm)
B	Si(001)/Cu (100 nm)/Fe_2O_3 (200 nm)
C	Si(001)/Al (40 nm)/Fe_2O_3 (200 nm)
D	Si(001)/Fe_2O_3 (20 nm)/Al (7 nm)/Fe_2O_3 (20 nm)/Cu (10 nm)/ Fe_2O_3 (20 nm)/Cu (10 nm)

In this paper, we present a new method for synthesizing Fe nanoparticles with electron beam deposition from Fe_2O_3 source. The main advantage of using electron beam deposition over other deposition techniques is the capability of controling the thickness of the film deposited without the presence of reactive ambient gases. We have investigated the role of surface states in determining the conditions for the fabrication of constant stoichiometric Fe_2O_3 films by depositing it on various templates. We observed that the enthalpy of formation of various oxides plays an important role in determining the formation of Fe nanoparticles at the interface between the template and the Fe_2O_3 films. Fe nanoparticles formation were observed when Fe_2O_3 was deposited directly on Si(001) substrate or on Si(001) with Al buffer layer.

2. Experimental Details

Fe_2O_3 films were deposited using electron beam onto Si(001) substrate. The base pressure was maintained at 3×10^{-7} torr. The Si(001) substrates were ultrasonically cleaned in acetone for 30 min, and were then rinsed in isopropanol. Fe_2O_3 films were grown on various templates as shown in Table 1. During deposition, the Fe_2O_3 source is decomposed at high temperature. Depending on the substrate, the recombination process is dependent on the enthalpy values of the possible products that can be formed. For example, when Fe_2O_3 is deposited directly on Si(001) substrate, the formation of SiO_2 is favored leaving behind Fe nanoparticles at the interface.

X-ray Photoelectron Spectroscopy (XPS) was used to determine the relative amounts of Fe and Fe oxides present in the deposited film. XPS depth profile analysis was performed on a Physical Electronics Quantum 2000 Scanning ESCA Microprobe equipped with a monochromitized Al Kα source ($h\nu = 1486.6$ eV). The depth profile analysis of Fe 2p, O 1s and Si 2p for 200 nm Fe_2O_3 films was acquired with pass energy of 93.9 eV at 0.2 eV step size and Ar^+ beam energies of 1 kV raster 3 mm $\times$ 3 mm with calibrated sputter rate of 16 Å/min. The intensities for all the XPS spectra reported here have been normalized for comparison and were calibrated against C 1s peak (284.8 eV) of adventitious carbon. A 200.0 μm X-ray beam size was used for all acquisitions at take-off angle 45°. Transmission Electron Microscopy (TEM) was carried out to verify the presence of Fe nanoparticles on sample D. Likewise, X-ray diffraction was used to determine the relative crystal orientations in the deposited films. We characterized the magnetic properties of the deposited films using a Vibrating Sample Magnetometer (VSM).

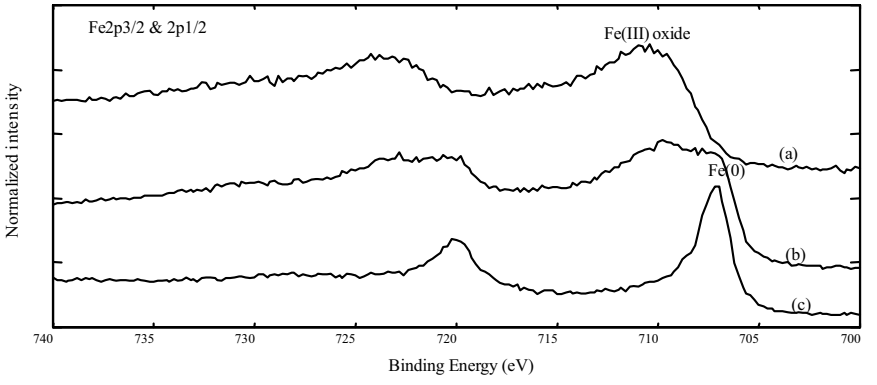

(a)

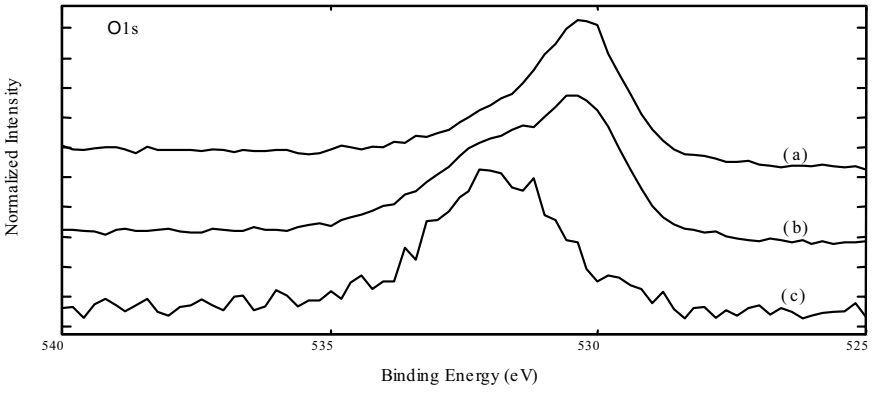

(b)

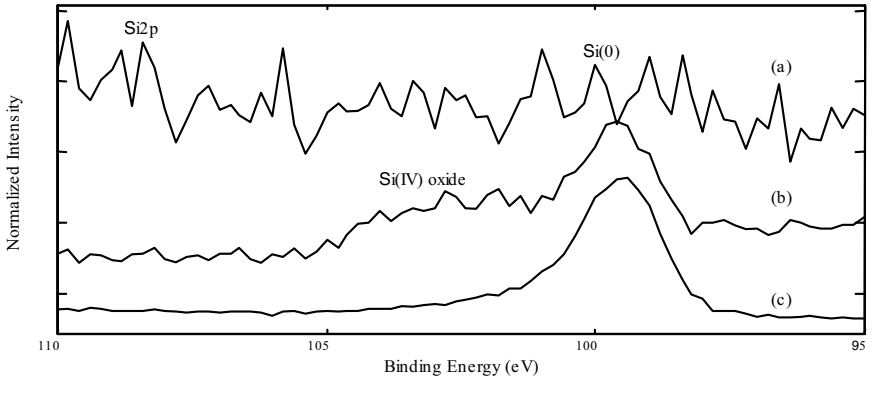

(c)

Fig. 1. XPS spectra for Fe 2p, O 1s and Si 2p core levels taken from sample A, a 200-nm Fe_2O_3 film deposited directly on Si(001) substrate. (a) "As-received"; (b) after 35 min sputtering; and (c) after 40 min sputtering during depth profile analysis.

3. Results and Discussion

Figure 1 shows the XPS spectra for Fe 2p, O 1s and Si 2p core levels for (a) as-received; (b) after 35 min sputtering; and (c) after 40 min sputtering that are extracted from the depth profile for the sample without the copper buffer layer, i.e., sample A. We observed that the binding energy of Fe 2p3/2 for the "as-received" surface is at 710 eV, which is associated with Fe(III) oxide; and the associated O 1s peak has binding energy of 530 eV. Not surprisingly, no Si peak is detected on the "as-received" surface. However, after 35 min of sputtering, a small "shoulder" is observed on the Fe 2p3/2 spectra at a binding energy of about 707 eV. A similar observation is found for the O 1s peak, whereby one "small bump" is seen at a higher binding energy (about 532 eV). In addition to this, a Si signal is also detected, which shows a mixed state containing both elemental silicon (99 eV) and silicon oxide (103 eV). Further sputtering to 40 min reveals only the presence of metallic Fe. A trace amount of oxygen is still detected at binding energy about 532 eV, which is probably attributed to a residue of silicon dioxide. During electron beam deposition, a beam of electrons falls on the target material (Fe_2O_3) and decomposes it into Fe and free oxygen. If one compares the enthalpy of formation for Fe(III) oxide and Si(IV) oxide, we noticed that the formation of Si(IV) oxide is much easier than the formation of Fe(III) oxide. This suggests that there is a continuous competition at the template interface for oxygen to react and form an oxide. Due to the lower enthalpy of formation of Si(IV) oxide, free oxygen at the interface readily reacts with Si and forms Si(IV), leaving behind metallic Fe(0), resulting in the nonuniform growth of Fe_2O_3 film.

The depth profile analysis was repeated for sample B, i.e. Fe_2O_3 deposited on Cu buffer layer, to study the stoichiometry of the Fe_2O_3 deposited. Figure 2 shows the Fe 2p, O 1s and Si 2p core levels spectra from similar sputtering intervals to those presented in Fig. 1. There is no obvious chemical shift of the Fe 2p peaks for both "as-received" and after sputtering. The binding energy of Fe 2p3/2, at about 710 eV, is consistent with Fe(III) oxide. The binding energies for its associated O 1s peaks, 530 eV are also consistent with Fe(III) oxide. This suggests that the stoichiometry of the Fe_2O_3 film remains unchanged throughout the 40 min of sputter etching using energized Ar^+ ions. This observation is in agreement with the theory of surface oxidation, whereby the enthalpy of formation of CuO, as shown in Table 2, is much higher than Fe(III) oxide. Therefore, at the interface, Fe(III) oxide is formed more easily than CuO.

In another experiment, we deposited a buffer layer of 40 nm of metallic aluminum (Al) onto Si(001). XPS depth profile analysis shows that Fe nanoparticles are formed in a similar way to those formed on the Si substrate, resulting in the formation of Al_2O_3 at the interface between the Fe nanoparticles and the metallic Al which was originally deposited. This can be attributed to the lower enthalpy of formation of Al_2O_3 when compared to the enthalpy formation of Fe(III) oxide as shown in Table 2.

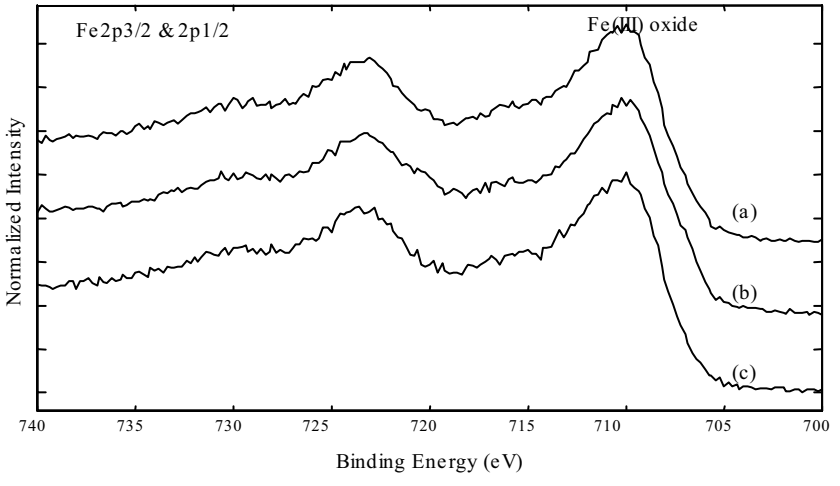

(a)

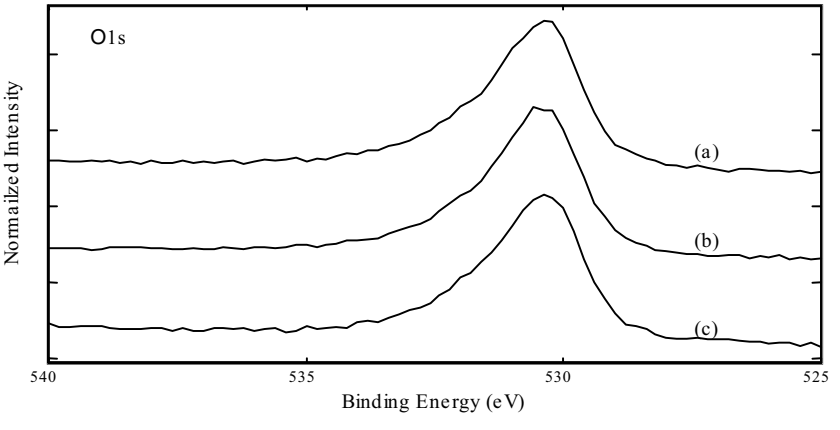

(b)

Fig. 2. XPS spectra for Fe 2p and O 1s core levels taken from sample B, 200 nm of Fe_2O_3 deposited on a Si(001) substrate with a 100-nm copper buffer layer. (a) "As-received"; (b) after 35 min sputtering; and (c) after 40 min sputtering during depth profile analysis.

Table 2. Enthalpy values for various oxides.

Oxide	Enthalpy (kJ/mole)[10]
Fe_2O_3	−822.30
SiO_2	−910.70
CuO	−155.00
Al_2O_3	−1674.00

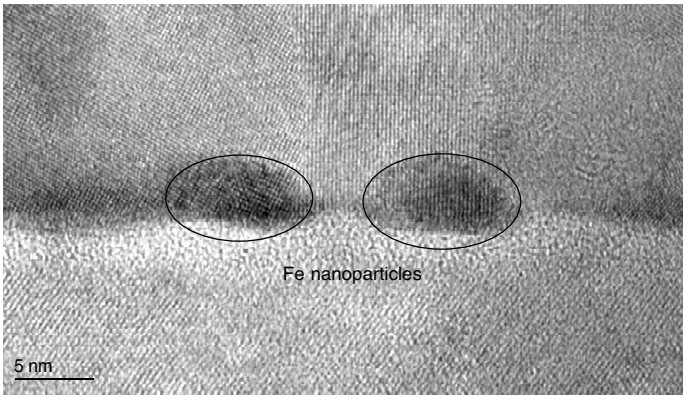

Fig. 3. HRTEM micrograph showing Fe nanoparticles near the Si(001) and Fe_2O_3 interface.

We have also investigated, using Transmission Electron Microscopy, the microstructure and size distribution of the Fe nanoparticles in sample D, a multilayer structure deposited on Si(001) substrate at 50°C. The Si substrate is at the bottom, with the Fe_2O_3 layer above in which the individual Fe_2O_3 grains can be seen. Between the Fe_2O_3 layer and the Si is a row of smaller grains adjacent to the Fe_2O_3 and an amorphous layer adjacent to the substrate. Figure 3 shows the HRTEM micrograph of the two grains of Fe near Si(001):Fe_2O_3 interface. These oval shaped nanoparticles are found to be of (100) orientation. Analysis of the lattice fringe spacing of individual grains in this high resolution image showed that the particles adjacent to the Fe_2O_3 which are Fe nanoparticles have a grain size of about 5 nm. Between the Fe nanoparticles and the Si substrate is an amorphous layer, which we deduce to be SiO_2.

Figure 4 shows the XRD graphs for (a) sample A and (b) sample B. A low intensity peak at 43.33° can be seen corresponding to (400) orientation for Fe_2O_3 in Fig. 4(a). The XRD pattern for the as-obtained sample reveals that the Fe nanoparticles between the oxide layers (SiO_2 and Fe_2O_3) are amorphous in the sense of the X-Ray Diffraction[9] (with a grain size lower than 5 nm, diffraction effects are diffuse and close to the background noise, therefore, when the crystalline coherence is lower than this value, the material is considered as amorphous in the sense of the X-ray diffraction). However, there is a marked increase in the intensity of (400) peak when Fe_2O_3 is deposited on Cu buffer layer as shown in Fig. 4(b); suggesting the growth of Fe_2O_3 to be highly crystalline in nature and showing no presence of metallic Fe. We also observed low intensity peaks for other orientations which can be attributed to Fe_2O_3.

The magnetic properties of Fe_2O_3 grown on Si(001) substrate with and without a Cu buffer layer were confirmed using VSM. Figure 5 shows the representative M–H loops for samples A and B. The low coercivity of 225 Oe for sample A is attributed to the presence of soft Fe nanoparticles at the interface which decreases the overall coercivity. However, the presence of Cu buffer layer forbids the formation

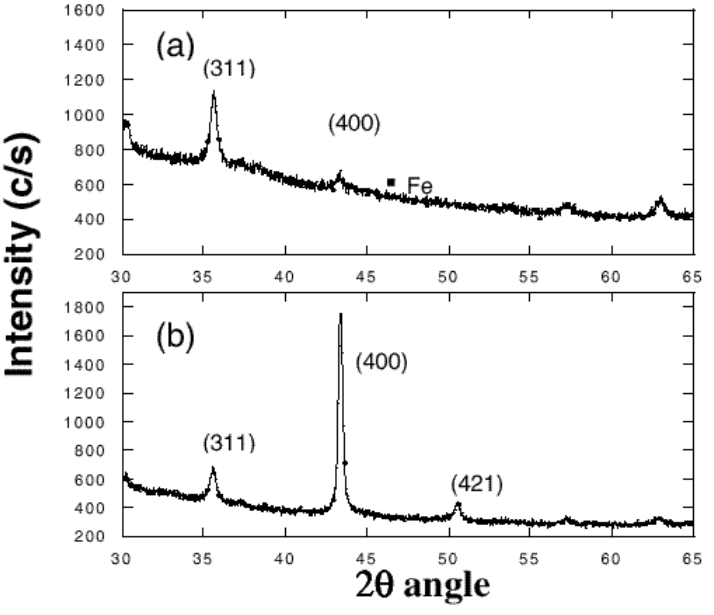

Fig. 4. XRD patterns for (a) 200 nm of Fe_2O_3 deposited directly on a Si(001) substrate and (b) 200 nm of Fe_2O_3 deposited on 100 nm of Cu buffer layer.

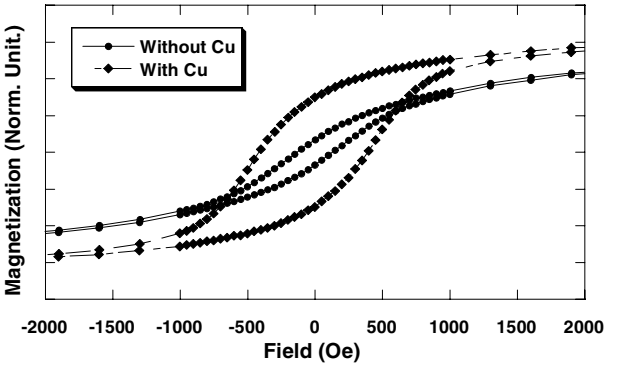

Fig. 5. M–H loops from 200 nm of iron oxide film deposited on Si(001) substrate and on 100 nm Cu buffer layer.

of Fe nanoparticles due to the high enthalpy energy of CuO, thus growing constant stoichiometric Fe_2O_3 film with high coercivity of 372 Oe for sample B.

4. Conclusion

We have developed a new technique for synthesizing Fe nanoparticles based on a redox reaction. We have fabricated crystalline Fe_2O_3 layers on Cu templates. The enthalpy of formation of oxides is the dominant factor which determines the forma-

tion of Fe nanoparticles and the crystallinity of Fe_2O_3 films. For Fe_2O_3 deposited directly onto Si and on Al buffer layer, Fe nanoparticles are found to form because the enthalpy formation of SiO_2 and Al_2O_3 is lower than that of Fe_2O_3. Conversely, for Fe_2O_3 deposited onto a Cu buffer layer, the formation of Fe nanoparticles is forbidden, thus growing crystalline Fe_2O_3 films because the enthalpy of formation for CuO is greater than the enthalpy of formation for Fe_2O_3.

References

1. M. Nastasi, D. M. Parkin and H. Gleiter, *Mechanical Properties and Deformation Behavior of Materials Having Ultra-Fine Microstructures* (Kluwer, Dordrecht, 1993).
2. A. S. Edelstein and R. C. Cammarata, *Nanomaterials*: *Synthesis*, *Properties and Applications* (IOP, London, 1996).
3. C. Hayashi, R. Uyeda and A. Tasaki, *Ultrafine Particles*: *Explanatory Science and Technology* (Noyes, Park Ridge, New Jersey, 1997).
4. Z. L. Wang, *Characterization of Nanophase Materials* (Wiley-VCH Verlag Gmbh, Federal Republic of Germany, 2000).
5. G. C. Hadjipanayis and G. A. Prinz, *Science and Technology of Nanostructured Magnetic Materials* (Plenum, New York, 1991).
6. F. Jorgenson, *The Complete Handbook of Magnetic Recording* (McGraw Hill, New York, 1996).
7. S. Gangopadhyay and G. C. Hadjipanayis, *J. Phys.* **70**, 5888 (1991).
8. Y. Li, P. Xiong and S. Von Molnar, *J. Phys.* **80**, 4644 (2002).
9. C. Del Bianco *et al.*, *J. Appl. Phys.* **84**, 2189 (1998).
10. M. W. Chase, *Tr. NIST-JANAF Thermochemical Tables*, 4th edn., J. Phys. Chem. Ref. Data, Monograph 9, 1998.